HAL
open science

Deformable two-dimensional photonic crystal slab for cavity optomechanics

T. Antoni, A. G. Kuhn, T. Briant, P.-F. Cohadon, A. Heidmann, R. Braive, A. Beveratos, I. Abram, L. Le Gatiet, I. Sagnes, et al.

To cite this version:

T. Antoni, A. G. Kuhn, T. Briant, P.-F. Cohadon, A. Heidmann, et al.. Deformable two-dimensional photonic crystal slab for cavity optomechanics. Optics Letters, 2011, 36 (17), pp.3434. hal-00605111

HAL Id: hal-00605111

https://hal.science/hal-00605111v1

Submitted on 30 Jun 2011

HAL is a multi-disciplinary open access archive for the deposit and dissemination of scientific research documents, whether they are published or not. The documents may come from teaching and research institutions in France or abroad, or from public or private research centers.

L'archive ouverte pluridisciplinaire **HAL**, est destinée au dépôt et à la diffusion de documents scientifiques de niveau recherche, publiés ou non, émanant des établissements d'enseignement et de recherche français ou étrangers, des laboratoires publics ou privés.

Deformable two-dimensional photonic crystal slab for cavity optomechanics

Thomas Antoni,* Aurélien G. Kuhn, Tristan Briant, Pierre-François Cohadon, and Antoine Heidmann
Laboratoire Kastler Brossel, UPMC-ENS-CNRS, Case 74, 4 place Jussieu, F75252 Paris Cedex 05, France
**Corresponding author: thomas.antoni@spectro.jussieu.fr*

Rémy Braive, Alexios Beveratos, Izo Abram, Luc Le Gratiet, Isabelle Sagnes, and Isabelle Robert-Philip
Laboratoire de Photonique et Nanostructures LPN-CNRS, UPR-20, Route de Nozay, 91460 Marcoussis, France

We have designed photonic crystal suspended membranes with optimized optical and mechanical properties for cavity optomechanics. Such resonators sustain vibration modes in the megahertz range with quality factors of a few thousand. Thanks to a two-dimensional square lattice of holes, their reflectivity at normal incidence at 1064 nm reaches values as high as 95 %. These two features, combined with the very low mass of the membrane, open the way to the use of such periodic structures as deformable end-mirrors in Fabry-Perot cavities for the investigation of cavity optomechanical effects.

Cavity optomechanics based on mechanically deformable optical microcavities has attracted a lot of attention over the past few years in view of applications in sensing and monitoring of mechanical motion. A fundamental motivation behind such work resides in the possibility of optically cooling the mechanical motion, in view of reaching the quantum ground state of the mechanical system [1, 2]. Downsizing the mechanical resonator allows one to enhance the optomechanical coupling by reducing the effective mass of the vibration modes. Among the various nanomechanical oscillators presently investigated, photonic crystal slabs may be good candidates, in particular due to the versatility of their optical properties combined with their very low mass. For instance, a "defect" in a planar one- or two-dimensional periodic dielectric structure can offer a strong confinement for both photons and phonons simultaneously inside a very small volume, thus exhibiting a strong optomechanical coupling [3, 4]. The optomechanical response of two coupled membranes, each pierced as a perfect two-dimensional periodic dielectric structure sustaining band-edge Bloch modes, has also been investigated [5].

In this paper, we present a new optomechanical device based on a suspended photonic crystal membrane that can be used as a deformable end-mirror in a Fabry-Perot cavity optomechanical system. We investigate both its mechanical response (frequencies and quality factors of the vibration modes) and its optical response (reflectivity at normal incidence).

The photonic crystal consists of an InP slab pierced with a square lattice of holes. The whole structure is grown by metal-organic vapor phase epitaxy on an InP substrate, starting with a 1 μm InGaAs sacrificial layer and then the InP slab layer. Inductively coupled plasma etching of the photonic crystal is performed on the top InP layer using a SiN hard mask defined by electron-beam lithography and dry etching. To suspend the InP membrane, the sacrificial layer under the membrane is removed by selective wet etching [6].

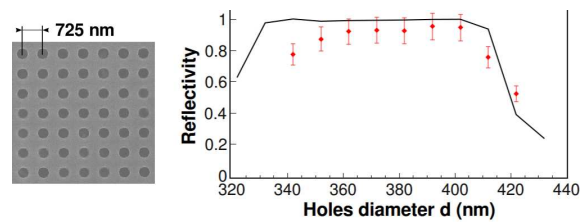

FIG. 1. Left: Scanning electron microscope close-up view of the photonic crystal structure. Right: measured (red dots) and simulated (black curve) reflectivity at 1064 nm of a $10 \times 20 \times 0.26$ μm^3 fully clamped photonic crystal.

We were able to suspend membranes as large as 30×30 μm^2, using several clamping solutions as described in the following. We have optimized the photonic crystal structure in order to maximize its optical reflectivity at normal incidence: transmission through the slab and in-plane losses can be canceled out by coupling the incident radiation to Bloch modes with a flat dispersion curve at the Γ point of the Brillouin zone. Moreover, it is desirable to design a mirror with broadband reflectivity so as to overcome fluctuations of the spectral position of the high-reflectivity zone, which may be due to defects and inhomogeneities introduced during the slab processing. As suggested in [7], this can be obtained by coupling two non-degenerate but overlapping slow Bloch modes close to the Γ point with the radiated modes in the vertical direction. Finite Difference Time Domain MEEP code [8] and eigenmode solver [9] MPB have been used to determine adequate parameters for the photonic crystal slabs in order to reach a near unity reflectivity over more than 50 nm around 1064 nm. The simulations are performed for an infinite structure, taking into account the evanescent coupling and cavity effects with the underlying substrate.

Fully clamped 30×30 μm^2 samples with a thickness

of 260 nm have been processed to measure the slab's reflectivity as a function of the optical wavelength by use of a Fourier transform infrared spectroscopy setup. The corresponding spectral behavior is shown in Figure 2 for a photonic crystal structure corresponding to a square array of holes, with a period of 725 nm and different diameters (see Figure 1). The measured band edges well coincide with reflectivity calculations, in particular the cut-off wavelengths of the large plateau around 1064 nm, and the resonance about 1010 nm. The spectral displacement of this resonance with increasing hole diameters is also well reproduced. The dip in the middle of the large plateau, mostly visible in the calculated and measured spectra but with a depth that depends on the hole diameter, is a consequence of the splitting between the two underlying Bloch modes. Note that due to finite size effects and optical diffraction, as well as to alignment and focusing difficulties, the presented results are arbitrary normalized so that absolute values of the curves are irrelevant. The reduced visibility of the experimental reflectivity may be due as well to finite size effects, as the beam waist is of the order of the photonic crystal area, or to non-uniform hole diameters over the membrane (resulting from proximity effects during the electron beam lithography of such large photonic crystal surfaces [10]), or to the roughness of the substrate behind the membrane, hence distorting the photonic crystal resonances.

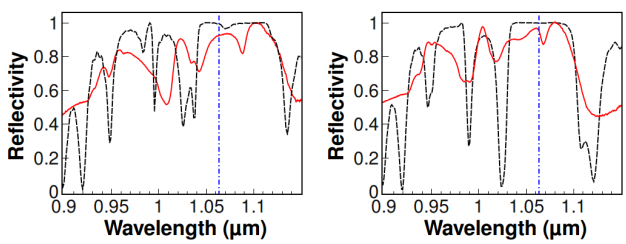

FIG. 2. Normalized experimental (red solid line) and simulated (black dashed line) reflectivities as a function of the wavelength, for a $30 \times 30 \times 0.26\,\mu\text{m}^3$ fully clamped photonic crystal membrane with holes diameters of 372 nm (left) and 392 nm (right).

Cavity operation of such membranes requires a very small beam waist to minimize clipping loss. As a consequence the reflectivity may be affected by the resulting beam divergence, about 6° for a waist of 3 μm. To investigate this effect, and also to measure an absolute value of the reflectivity, we have used a small $10 \times 20\ \mu\text{m}^2$ fully clamped membrane and focused a laser beam to a waist as small as 2.5 μm with a microscope objective (0.65 numerical aperture). In addition, we have measured the dependence of the reflectivity on the hole diameter. Experimental results obtained by comparing the reflected power to the one reflected by a 99.94% commercial mirror are shown in Figure 1. They are in good agreement with FDTD simulations, demonstrating that divergence effects do not limit the reflectivity. The absolute reflectivity reaches values as high as $95\% \pm 8\%$.

For the investigation of the mechanical response of the membrane, we have built a Michelson-like interferometer in which the membrane is the end-mirror in one of the arms. The light from a 1064 nm Nd:YAG laser source is focused on the membrane with the microscope objective, down to a beam waist of 2.5 μm. The membrane position is adjusted thanks to a motorized 3-axis translation stage. The setup is inserted into a vacuum chamber pumped down to 10^{-4} mbar.

The interference between the two arms is monitored by a photodiode and sent to a network analyzer which is also used to activate the resonator via a piezoelectric stack. On the aforementioned membranes, typical results show mechanical modes with resonance frequencies in the megahertz range and with quality factors about 1000, due to clamping losses. We consequently have tried different geometries and best results have been obtained with $10 \times 20\ \mu\text{m}^2$ suspended membranes, with a thickness of 210 nm. The membrane is suspended by four bridges with optimized position, length and width (see inset in Fig. 3) [11]: they are symmetrically located 5.9 μm from the center of the membrane, at the node of the fundamental longitudinal mode (0,0), as computed with Comsol Multiphysics. We have tested samples with auxiliary bridges length ranging from 2 μm to 12 μm, and with a width down to 0.5 μm.

The spectrum of the mechanical response obtained with a membrane suspended by 8 μm-long auxiliary bridges is shown in Figure 3. It displays six mechanical modes whose frequencies $\Omega_\text{m}/2\pi$ are in the megahertz range, as expected from finite-element simulations, with the mode of interest about 2.5 MHz. The estimated effective mass of this mode is of the order of 150 pg.

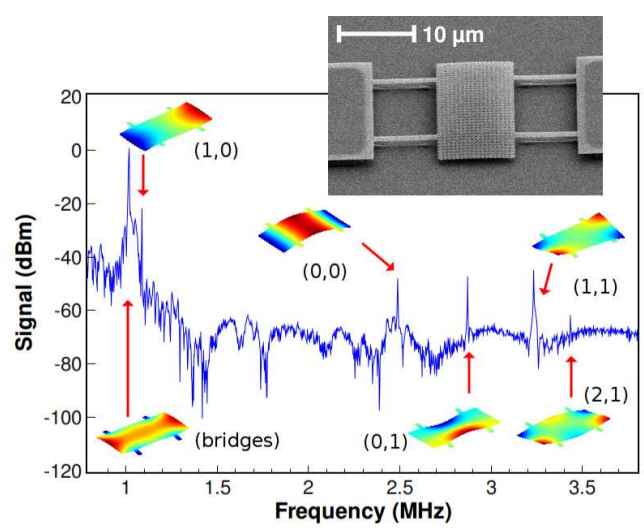

FIG. 3. Displacement spectrum of a $10 \times 20 \times 0.21\,\mu\text{m}^3$ photonic crystal membrane, clamped by four 8 μm-long and 1 μm-wide auxiliary bridges, as shown in the scanning electron microscope image. The simulated vibration profile is shown for each mechanical mode.

The quality factors Q_m of the mechanical modes are in-

ferred via a ring-down technique, by measuring the decay time of the vibration mode after switching off the membrane actuation at the resonance frequency. Quality factors ranging from 2 000 to 10 000 are obtained, without relevant dependence on the observed mode. We have investigated various dissipation mechanisms that may limit these quality factors. For instance, we have checked that $Q_{\rm m}$ does not depend on pressure below 10^{-1} mbar, ruling out air viscous damping and the well known squeezed-film damping[12]. Using Zener model [13], we have estimated that thermoelastic damping is negligible as well. Another mechanism that can be eliminated is the clamping losses corresponding to dissipation into the substrate, since $Q_{\rm m}$ has no clear dependence on the length or the position of the four auxiliary bridges.

Two dominant dissipation channels can consequently be foreseen in our system. The first one corresponds to surface effects [14, 15], whose impact goes up for increasing surface-to-volume ratio, estimated to $10\,\mu\mathrm{m}^{-1}$ (or 1 over 500 atoms) with our structures. Another loss mechanism is related to crystal defects of the membrane, either induced in the bulk material during processing, or due to a non-intentional residual doping, estimated at about $10^{17}\,\mathrm{cm}^{-3}$ [16, 17].

Note that the bending of the membrane distinguishable in Figure 3 is due to residual stress and yields to a radius of curvature of about $100\,\mu$m. This is not an issue for the design of a cavity since coupling mirrors with smaller radius of curvature are achievable [18].

Large optomechanical effects are expected by combining such mechanical properties to high optical reflectivities, making these photonic-crystal slabs promising candidates for cavity optomechanics experiments. As an example, the shot-noise limited displacement sensitivity with a single-ended Fabry-Perot cavity would already be large enough to observe the Brownian and quantum motions of the membrane. It is given by :

$$\delta x_{\rm shot} = \frac{\lambda}{16\mathcal{F}\sqrt{\overline{I}_{\rm in}}}\frac{T+L}{T}, \qquad (1)$$

where $\mathcal{F}$ is the cavity finesse, T the transmission of the coupling mirror and L the cavity losses (including the membrane reflectivity). Based on our experimental results, we find $\delta x_{\rm shot} \simeq 2\times10^{-17}$ m/$\sqrt{\rm Hz}$ for realistic parameters: incident power $P_{\rm in} = (hc/\lambda)\,\overline{I}_{\rm in} = 5$ mW, $\mathcal{F} \simeq 100$, $L = 5\%$, and $T \simeq 1\%$. This value is four orders of magnitude smaller than the Brownian motion amplitude of the fundamental mode at 300 K ($\delta x_T = \sqrt{2Q_{\rm m}k_BT/(M\Omega_{\rm m}^3)} \simeq 2\times10^{-13}$ m/$\sqrt{\rm Hz}$), and of the same order of magnitude as its zero-point motion ($\delta x_T \simeq 5\times10^{-17}$ m/$\sqrt{\rm Hz}$ at $T \lesssim 150\,\mu$K).

Further improvement of the mechanical quality factors may allow the experimental demonstration of the ground state of these resonators, by performing cryogenic and laser coolings of the membrane either used as an end-mirror in a Fabry-Perot cavity, or as a high-reflectivity membrane in "membrane-in-the-middle" setups [19].

This research has been partially funded by the FP7 Specific Targeted Research Projects QNems, and by the C'Nano Ile-de-France project Naomi.

[1] O. Arcizet, P.-F. Cohadon, T. Briant, M. Pinard, and A. Heidmann, Nature **444** (2006).
[2] A. Schliesser, P. Del'Haye, N. Nooshi, K. J. Vahala, and T. J. Kippenberg, Phys. Rev. Lett. **97**, 243905 (2006).
[3] M. Eichenfield, J. Chan, R. Camacho, K. J. Vahala, and O. Painter, Nature **462**, 78 (2009).
[4] E. Gavartin, R. Braive, I. Sagnes, O. Arcizet, A. Beveratos, T. J. Kippenberg, and I. Robert-Philip, arXiv:1011.6400 .
[5] Y.-G. Roh, T. Tanabe, A. Shinya, H. Taniyama, E. Kuramochi, S. Matsuo, T. Sato, and M. Notomi, Phys. Rev. B **81**, 121101 (2010).
[6] A. Talneau, K. H. Lee, S. Guilet, and I. Sagnes, Appl. Phys. Lett. **92**, 061105 (2008).
[7] S. Boutami, B. Benbakir, X. Letartre, J. L. Leclercq, P. Regreny, and P. Viktorovitch, Opt. Express **15**, 12443 (2007).
[8] A. F. Oskooi, D. Roundy, M. Ibanescu, P. Bermel, J. D. Joannopoulos, and S. G. Johnson, Comp. Phys. Comm. **181**, 687 (2010).
[9] S. G. Johnson and J. D. Joannopoulos, Opt. Express **8**, 173 (2001).
[10] C. F. R. Mateus, M. C. Y. H. L. Chen, C. J. Chang-Hasnain, and Y. Suzuki, IEEE PTL **16**, 1676 (2004).
[11] G. D. Cole, I. Wilson-Rae, K. Werbach, M. R. Vanner, and M. Aspelmeyer, Nat. Commun. **2**, 231 (2011).
[12] C. Zhang, G. Xu, and Q. Jiang, Journ. Micromech. Microeng. **14**, 1302 (2004).
[13] R. Lifshitz and M. L. Roukes, Phys. Rev. B **61**, 5600 (2000).
[14] J. Gaspar, V. Chu, and J. P. Conde, Appl. Phys. Lett. **84**, 622 (2004).
[15] X. Liu, J. F. Vignola, H. J. Simpson, B. R. Lemon, B. H. Houston, and D. M. Photiadis, J. Appl. Phys. **97**, 023524 (2005).
[16] K. L. Ekinci and M. L. Roukes, Rev. Sci. Instrum. **76**, 061101 (2005).
[17] P. Mohanty, D. A. Harrington, K. L. Ekinci, Y. T. Yang, M. J. Murphy, and M. L. Roukes, Phys. Rev. B **66**, 085416 (2002).
[18] D. Hunger, T. Steinmetz, Y. Colombe, C. Deutsch, T. W. Hänsch and J. Reichel, New J Phys **12**, 065038 (2010).
[19] J. D. Thompson, B. M. Zwickl, A. M. Jayich, F. Marquardt, S. M. Girvin, and J. G. E. Harris, Nature **72**, 452 (2008).